논문 2010-47SD-7-3

Mach-Zehnder 광변조기의 양방향 변조를 이용한 새로운 광섬유격자 센서 검출 방법

(A Novel Fiber Bragg Grating Sensing Interrogation Method Using Bidirectional Modulation of a Mach-Zehnder Electro-Optical Modulator)

모 만 개*, 반 재 경**

(Wankai Mao and Jae-Kyung Pan)

요 약

본 논문에서는 Mach-Zehnder 광변조기의 양방향 변조를 이용하는 새로운 광섬유격자 센서 검출 방법을 제안하고 실험을 통하여 그 유용성을 밝힌다. 제안한 구조는 광대역 광원, 광섬유격자, Mach-Zehnder 광변조기, chirped 광섬유격자, 그리고 광검출기로 구성된다. 실험을 통하여 제안한 구조의 전달함수를 구하고, 505 MHz에서 525 MHz까지 주파수 영역에서 10개의 다른 파장을 가진 광에 대한 FSR(free spectral range)의 변화로부터 시간지연을 계산한다. 구한 결과로부터 광의 파장 변화에 따른 시간지연이 12.9 ps/0.2 nm 값을 가지면서 매우 선형적임을 알 수 있다. 이러한 결과는 광섬유격자를 이용한 스트레인 또는 온도 센서에 이용할 수 있다.

Abstract

We have proposed and experimentally demonstrated a novel fiber Bragg grating (FBG) sensing interrogation method using bidirectional modulation of a Mach-Zehnder electro-optical modulator (MZ-EOM). The proposed structure consists mainly of a broadband light source (BBS), FBG, MZ-EOM, chirped fiber Bragg grating (CFBG), and photodetector (PD). We have obtained the transfer functions of the proposed structure and calculated the time delay from the change in the free spectral range (FSR) for ten wavelengths over the frequency range of 505 MHz to 525 MHz. The results show that the time delay and the wavelength variation have a good linear relationship with a gradient of 12.9 ps/0.2 nm, which can be usefully applied to FBG strain or temperature sensors and other multiplexed sensor applications.

Keywords : Sensing interrogation method, Fiber Bragg grating (FBG), Chirped fiber Bragg grating (CFBG), Mach-Zehnder electro-optical modulator (MZ-EOM), Bidirectional modulation

I. Introduction

The use of FBGs in sensor applications has been studied extensively for twenty years. FBGs are light weight, offer low power consumption and multiplexing capability, are resistant to electromagnetic waves interference, and offer high sensitivity to strain and temperature. FBG sensors, because of their small size, are ideally suited for health monitoring of smart structures since they can easily be embedded inside structural members[1]. Several FBG sensor interrogation systems which can be classified into passive detection and active detection have been reported[2]. The successful schemes include the scanning Fabry-Perot or

* 학생회원, ** 평생회원-교신저자, 전북대학교 전기공학과
(Department of Electrical Engineering, Chonbuk National University)
※ 이 논문은 2008년 정부(교육과학기술부)의 재원으로 한국연구재단의 지원을 받아 수행된 연구임 (D00307)
접수일자: 2010년3월9일, 수정완료일: 2010년6월21일

acoustic filters, tuning lasers and charge coupled device (CCD) spectrometers. Each of them has its own advantages, and commercial systems that make use of these techniques are now available.

Recently, FBG sensor interrogation systems employing MZ-EOM have started research attention due to the capability of MZ-EOM in handling fast signal processing speed. By adopting the fiber Sagnac-loop-based microwave photonic filtering, the high-frequency wavelength variation of a sensing FBG can be converted into the intensity change of the recovered RF signal[3]. An FBG interrogator, by using a dispersion compensation fiber, can convert the sensing wavelength variation measurement to time-domain measurement at a speed of the order of megasamples per second[4]. Bidirectional modulation of MZ-EOM has been used to find the optical fiber chromatic dispersion measurement[5]. In this paper, based on the microwave photonic technique and active detection, we have proposed and demonstrated a novel FBG sensing interrogation method using bidirectional modulation of an MZ-EOM.

II. Proposed Interrogation Structure and Operational Principle

As we know, the principle of FBG sensor is that the measured information is wavelength-encoded in the Bragg reflection of the grating. Especially, FBGs are sensitive to strain and temperature, then any applied strain or temperature shifts the resonance wavelength and this variation can be measured to calculate the strain change or amount of temperature applied. For example, the Bragg wavelength variation $\Delta\lambda_B$ resulting from a change of the applied strain ε_z at constant temperature is

$$\frac{\Delta\lambda_B}{\lambda_B} = (1 - p_e)\cdot\varepsilon_z \qquad (1)$$

where p_e is the effective strain-optic constant. Typically, the Bragg wavelength variation with strain is ~0.64 pm/με near the Bragg wavelength of 830 nm,

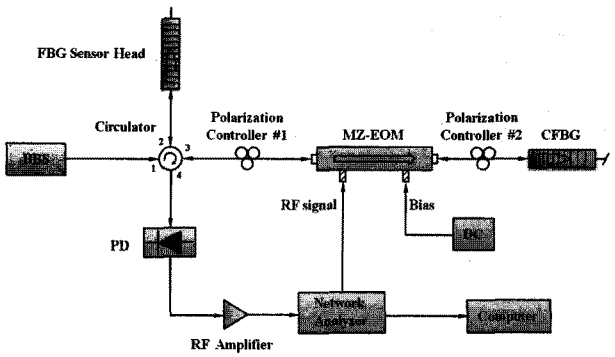

그림 1. 제안한 광섬유격자 센서 검출 구조
Fig. 1. Proposed FBG sensing interrogation structure.

~1 pm/με near 1300 nm, and ~1.2 pm/με near 1550 nm[6]. So, the primary work for the FBG sensor lies in the wavelength interrogation of the Bragg reflection. The general theory is to convert the wavelength variation measurement to other easily measured parameter, such as amplitude, phase or frequency.

Fig. 1 shows our proposed structure of a novel FBG sensing interrogation method, which consists mainly of a BBS, FBG, MZ-EOM, CFBG and PD. Light from BBS launches into port 1 of a four-port circulator, and is reflected by a sensing FBG in port 2. After passing through port 3 and the polarization controller #1, the light is modulated by an RF signal via the MZ-EOM with co-propagation i.e. propagation in the same direction as the light and as indicated by the arrow on the diagram of the MZ-EOM shown in Fig. 1. The unidirectional modulated light is reflected by the CFBG, passes through the polarization controller #2 again, and is modulated by an RF signal via the MZ-EOM with counter-propagation i.e. propagation in the opposite direction to the light and as indicated by the arrow on the diagram of the MZ-EOM shown in Fig. 1. The bidirectional modulated light is received by the

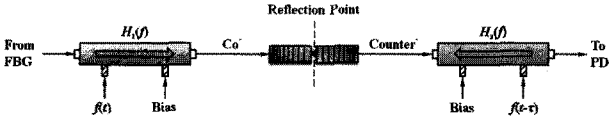

그림 2. MZ-EOM과 CFBG를 가진 구조의 양방향 변조 등가 모델
Fig. 2. Equivalent model of bidirectional modulation with an MZ-EOM and a CFBG.

PD and measured by the network analyzer (NA). The modulating process of bidirectional modulation in Fig. 1 can be considered in terms of the equivalent model shown in Fig. 2, which has two MZ-EOMs cascaded in series.

The travel time $\tau(\lambda)$ according to the wavelength of the proposed structure can be written as,

$$\tau(\lambda) = \tau_{fiber} + \tau_{CFBG}(\lambda) = \frac{2L_{fiber}}{v_g} + \frac{(\lambda_0 - \lambda)\cdot 2L_{CFBG}}{\Delta\lambda_{chirp}\cdot v_g} \quad (2)$$
$$(for \quad 2n_{eff}\Lambda_{short} < \lambda < 2n_{eff}\Lambda_{long})$$

where τ_{fiber} is the travel time spent in optical fiber between MZ-EOM and CFBG, τ_{CFBG} is the travel time spent in CFBG[7], L_{fiber} is the length of optical fiber between MZ-EOM and CFBG, L_{CFBG} is the grating length of CFBG, v_g is the group velocity of light in optical fiber, λ_0 is the central wavelength of CFBG, $\Delta\lambda_{chirp}$ is the chirped bandwidth of CFBG, n_{eff} is the effective index of the refraction of CFBG, Λ_{short} and Λ_{long} are the shortest period and the longest period in the CFBG, respectively. In Eq. (2), the wavelength of the sensing FBG has to be in the range of the chirped bandwidth of CFBG which is determined by the shortest and longest period in the CFBG.

The time delay $\Delta\tau$, which is the difference of the travel time for two wavelengths (λ_1, λ_2) can be expressed as,

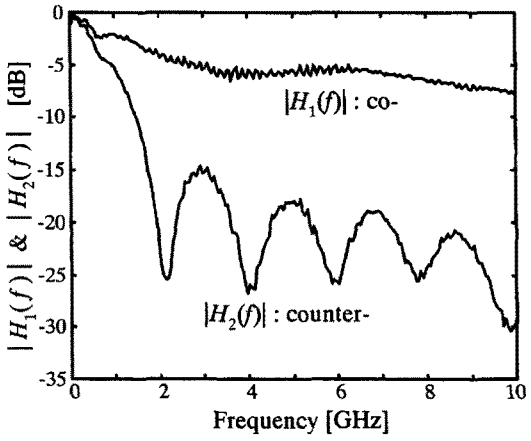

그림 3. MZ-EOM의 순방향과 역방향의 전달함수
Fig. 3. The transfer functions of co- and counter-propagating modulation of an MZ-EOM.

$$\Delta\tau = \tau(\lambda_2) - \tau(\lambda_1) = \frac{\Delta\lambda_B \cdot 2L_{CFBG}}{\Delta\lambda_{chirp}\cdot v_g} \quad (3)$$

where $\Delta\lambda_B$ is the wavelength variation of the sensing FBG. Eq. (3) shows that the time delay is proportional to the length of the CFBG and is inversely proportional to the chirped bandwidth of the CFBG. The wider chirped bandwidth of the CFBG with the shorter length makes increases the accuracy of the proposed structure. We can find the time delay according to the wavelength variation of the sensing FBG for the given CFBG.

In the course of propagation, the first MZ-EOM causes the right-handed propagating light in Fig. 1 to experience the co-propagating modulation by the RF signal $f(t)$. On the other hand, the second MZ-EOM causes the left-handed propagating light in Fig. 1 to experience the counter-propagating modulation by the RF signal $f(t-\tau)$. Fig. 3 shows the transfer functions of an MZ-EOM with a bandwidth of 10 GHz for co- and counter- propagating modulation.

Assuming that the modulation indices are very small, and with the biasing set at the quadrature point, we can obtain an expression for the output optical power $P_{out}(t)$ at the PD in the form,

$$\begin{aligned} P_{out}(t) &= \frac{P_{in}T_D}{4}[1 + m_1H_1(f)\cos 2\pi ft] \\ &\quad \cdot[1 + m_2H_2(f)\cos 2\pi f(t-\tau)] \\ &= \frac{P_{in}T_D}{4}[1 + m_1H_1(f)\cos 2\pi ft \\ &\quad + m_2H_2(f)\cos 2\pi f(t-\tau) \\ &\quad + m_1m_2H_1(f)H_2(f)\cos 2\pi ft \\ &\quad \cdot\cos 2\pi f(t-\tau)] \end{aligned} \quad (4)$$

where P_{in} is the input optical power, T_D is the coupling and optical transmission losses of the structure, m_1 and m_2 are the modulation indices of co-propagating and counter-propagating modulation, respectively, and $H_1(f)$ and $H_2(f)$ are the transfer functions for co-propagating and counter-propagating modulation of the MZ-EOM, respectively.

The DC and harmonic components in Eq. (4) are

eliminated at the PD and the NA because all vector NAs use a tuned-receiver (narrow-band) architecture to reject harmonic and spurious signals. Consequently, assuming that $m_1=m_2=m$, the total transfer function $H(f)$ measured at the NA can be written as,

$$H(f) = A_0[H_1(f)+e^{-j2\pi f\tau}H_2(f)] \quad (5)$$

where $A_0=mRG_mP_{in}T_D/4$, R is the responsivity of the PD, and G_m is the gain of the RF amplifier. The FSR is formed by the ripples in the transfer function which depends on the travel time in Eq. (5), and the travel time is related to the period of the ripples strongly[8]. For each wavelength, FSR can be expressed as,

$$FSR_\lambda = \frac{1}{\tau(\lambda)} \quad (6)$$

Using Eq. (2), (3), and (6), the travel time and the time delay can be calculated by measuring the change in the FSR according to the wavelength variation.

III. Simulation Analysis and Experiment Results

Fig. 4 shows simulation result of the FSRs for three different optical fiber lengths between the MZ-EOM and the CFBG over the modulation frequency range from 0 to 1000 MHz, assuming a sensing FBG with a central wavelength of 1550.0 nm, a CFBG with a central wavelength of 1550.5 nm, a grating length of 18.5 mm, and a chirped bandwidth of 3.0 nm. Obviously, as the optical fiber lengths increase, the FSRs reduce, as shown by the 0.5 m (red line), 2.0 m (blue dash line), and 8.0 m (green dot line).

The FSRs arising with an optical fiber length of 0.5 m for the different wavelengths in the sensing FBG of 1548.0 nm (blue line) and 1551.0 nm (green dash line) are shown in Fig. 5, for a chirped bandwidth in the CFBG of 3 nm. As the wavelength of the sensing FBG increases, the FSR also increases. It is helpful to distinguish the wavelength variation using a CFBG with wide chirped bandwidth over the high modulation frequency range, but the phenomenon of aliasing comes out quickly at the same time. Furthermore, the characteristic of two transfer functions $H_1(f)$ and $H_2(f)$ are utterly unlike except that the modulation frequency range is significantly lower than the bandwidth of the MZ-EOM, near a frequency of 500 MHz, as shown in Fig. 3.

For the experimental set-up shown in Fig. 1, we use a BBS with an output power of -13 dBm/nm around 1550 nm (Agilent 83438A), an MZ-EOM with a bandwidth of 10 GHz (Photline MXAN-LN-10), a CFBG with bandwidth of 2.880 nm and its grating length of 18.5 mm, a PD with bandwidth of 25 GHz

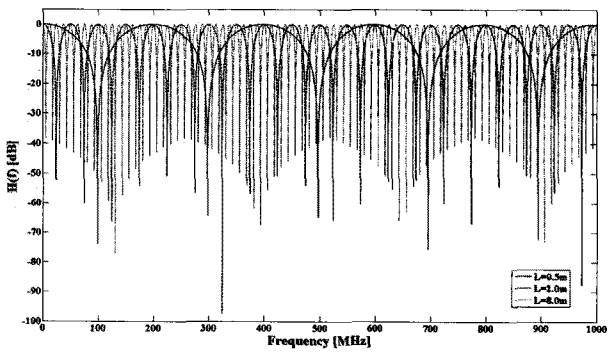

그림 4. MZ-EOM과 CFBG 사이의 광섬유 길이가 다른 경우(3 가지) FSR

Fig. 4. FSRs for three different optical fiber lengths between MZ-EOM and CFBG.

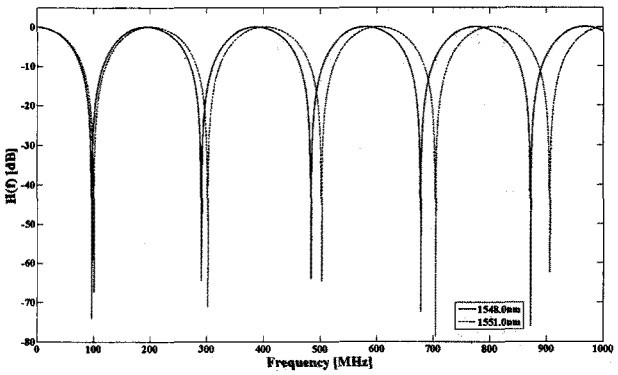

그림 5. 광섬유길이가 0.5 m일 때 CFBG의 chirped 대역폭을 고려한 FSR

Fig. 5. FSRs with the optical fiber length of 0.5 m considering the chirped bandwidth of CFBG.

(New Focus Model 1414), an RF amplifier with a gain of 18 dB (New Focus Model 1422), and an NA with an output RF signal of 1 dBm (Agilent N5230C). Practically, the DC bias voltage is set at 2.25 V, the optical fiber length between MZ-EOM and CFBG is 6.4 m, and the whole power loss of the arrangement is around -18 dB under the test conditions. Due to the problem of a weak optical signal, we use a tunable laser source with an output power of 8 dBm (Anritsu MG9638A) instead of the FBG sensing signal. This arrangement allowed us to demonstrate the feasibility of the proposed interrogation method. The simulation and experiment results of the transfer function $H(f)$ for ten wavelengths (from 1548.0 nm to 1549.8 nm in 0.2 nm steps) in the frequency range of 500 MHz to 550 MHz are shown in Fig. 6 (a) and (b), respectively.

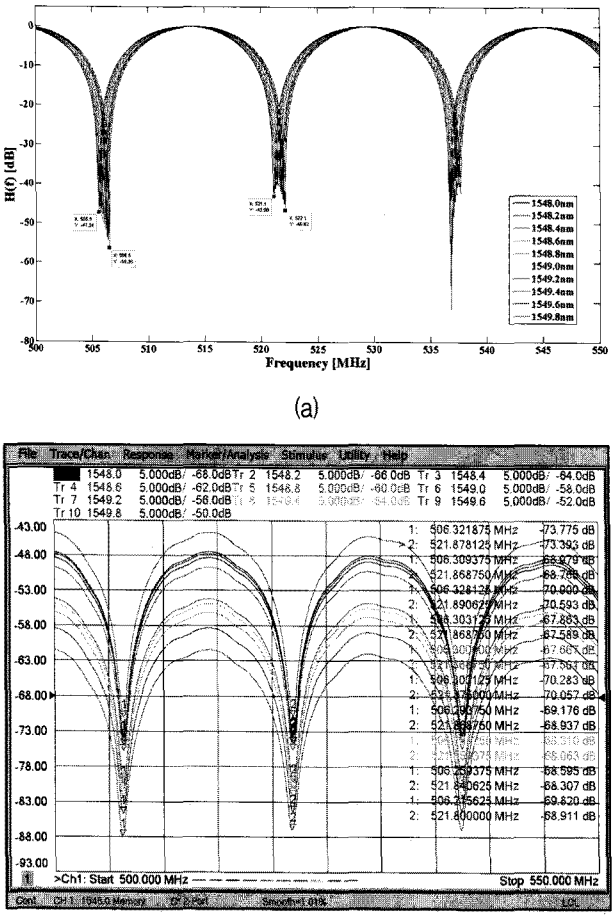

그림 6. 505 MHz에서 525 MHz까지 주파수 영역에서 10개의 다른 파장을 가진 광에 대한 전달함수 (a) 시뮬레이션 결과와 (b) 실험 결과

Fig. 6. Transfer function $H(f)$ for ten wavelengths in the frequency range of 500 MHz to 550 MHz (a) Simulation results and (b) Experiment results.

We can see that the simulation result and the measured result shown in Fig. 6 (a) and (b) are in good agreement. The travel time calculated from the experiment results using Eq. (6) provides the time delays for the ten different wavelengths used. Both of the FSR (blue triangle) and time delay (red square) variation as a function of wavelength are shown in Fig. 7. Depending on the orientation of CFBG in use, the FSR for each wavelength increases from 15.556250 MHz to 15.584375 MHz, corresponding to the travel time decreasing from 64.2828 ns to 64.1668 ns. We note that the relationship between the time delay and the wavelength variation is accurately

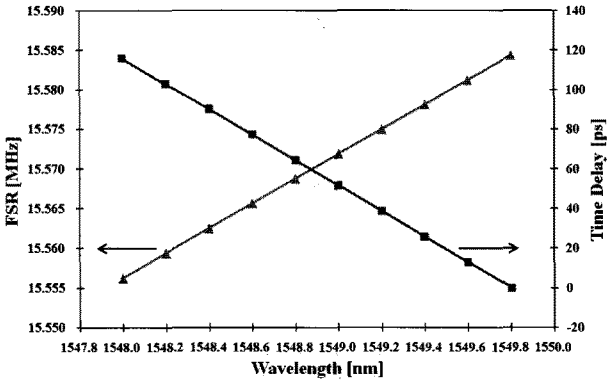

그림 7. 광의 파장 변화에 따른 FSR(푸른 삼각표시)과 시간 지연(붉은 사각표시)

Fig. 7. FSR(blue triangle) and time delay(red square) with the wavelength variation.

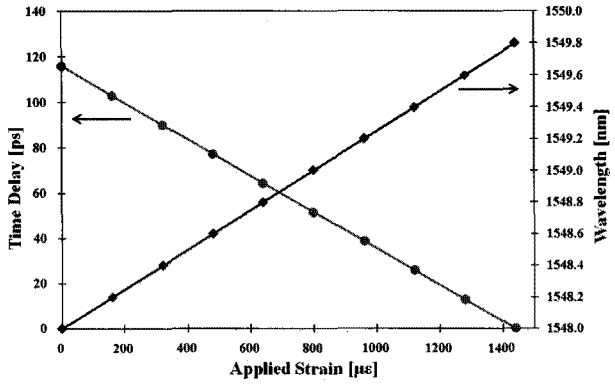

그림 8. 가해진 스트레인에 따른 시간 지연(푸른 원표시)과 파장변화(붉은 마름모표시)의 관계

Fig. 8. Time delay(blue circle) and wavelength(red diamond) with the applied strain.

linear with a gradient of 12.9 ps/0.2 nm. In order to improve the stability of proposed structure, three aspects should be necessary to pay attention to, the number of sampling points of NA (we used 16001 points), the temperature influence (keep temperature in 25℃), and the measuring times (repeat no less than 30 times). Moreover, combining Eq. (1) with the calculated results, we also can find the expected strain sensitivity at the sensing wavelength around 1550 nm is 0.2 nm variation in resonance wavelength per 167 με of the applied strain. Fig. 8 shows the relations of both of the time delay (blue circle) and wavelength (red diamond) with the applied strain.

IV. Conclusion

We have proposed and demonstrated a novel FBG sensing interrogation method using bidirectional modulation of an MZ-EOM. The transfer functions of the proposed method obtained by using a combination of simulation and experiment have been found, which are in good agreement. The calculated travel time from the transfer function results in the time delay for ten different wavelengths over the frequency range of 505 MHz to 525 MHz. The time delay and the wavelength variation that have a good linear relationship with a gradient of 12.9 ps/0.2 nm. The expected strain sensitivity at the sensing wavelength around 1550 nm is 0.2 nm variation in resonance wavelength per 167 με of the applied strain. Therefore, the proposed sensing interrogation method shows a potential for the FBG strain or temperature sensors and other multiplexed sensor applications.

References

[1] A. D. Kersey, M. A. Davis, H. J. Patrick, M. L. Blanc, K. P. Koo, C. G. Askins, M. A. Putnam, and E. J. Friebele, "Fiber Grating Sensors," J. Lightwave Technol., vol. 15, no. 8, pp. 1442-1463, Aug. 1997.

[2] S. Yin, P. B. Ruffin, F. T. S. Yu, Fiber Optic Sensors, CRC Press, 2008.

[3] H. Y. Fu, W. Zhang, C. B. Mou, X. W. Shu, L. Zhang, S. L. He, and I. Bennion, "High-Frequency Fiber Bragg Grating Sensing Interrogation System Using Sagnac-Loop-Based Microwave Photonic Filtering," Photon. Technol. Lett., vol. 21, no. 8, pp. 519-521, Apr. 2009.

[4] H. Y. Fu, H. L. Liu, X. Dong, H. Y. Tam, P. K. A. Wai, and C. Lu, "High-Speed Fiber Bragg Grating Sensor Interrogation Using Dispersion Compensation Fiber," Electron, Lett., vol. 44, no. 10, pp. 618-619, May 2008.

[5] K. S. Jeon, H. J. Kim, D. S. Kang, and J. K. Pan, "Optical Fiber Chromatic Dispersion Measurement Using Bidirectional Modulation of an Optical Intensity Modulator," Photon. Technol. Lett., vol. 14, no. 8, pp. 1145-1147, Aug. 2002.

[6] K. T. V. Grattan and B. T. Meggitt, Optical Fiber Sensor Technology, Chapman & Hall, 1998.

[7] R. Kashyap, Fiber Bragg Gratings, Academic Press, 1999.

[8] J. Capmany, B. Ortega, and D. Pastor, "A Tutorial on Microwave Photonic Filters," J. Lightwave Technol., vol. 24, no. 1, pp. 201-229, Jan. 2006.

저 자 소 개

모 만 개(학생회원)
2007년 중국 절강대학 전자공학과 졸업
2008년~현재 전북대학교 대학원 전기공학과 석사과정
<주관심분야 : 광섬유격자 센서, 광통신>

반 재 경(평생회원)-교신저자
1980년 연세대학교 전자공학과 졸업
1982년 연세대학교 대학원 전자공학과 공학석사
1987년 연세대학교 대학원 전자공학과 공학박사
1987년~현재 전북대학교 전기공학과 교수
<주관심분야 : 광통신 소자 및 시스템, 광 FBG 응용>